



# Quantitative Assessment of the Apical and Basolateral Membrane Expression of VEGFR2 and NRP2 in VEGF-A-stimulated Cultured Human Umbilical Vein Endothelial Cells

Esmeralda K. Bosma, Shahan Darwesh, Jia Y. Zheng, Cornelis J.F. van Noorden, Reinier O. Schlingemann, and Ingeborg Klaassen 

Ocular Angiogenesis Group, Department of Ophthalmology, Amsterdam UMC location University of Amsterdam, Amsterdam, The Netherlands (EKB, SD, JYZ, CJFVN, ROS, IK); Amsterdam Cardiovascular Sciences, Microcirculation, Amsterdam, The Netherlands (EKB, SD, JYZ, ROS, IK); Amsterdam Neuroscience, Cellular & Molecular Mechanisms, Amsterdam, The Netherlands (EKB, SD, JYZ, ROS, IK); Department of Genetic Toxicology and Cancer Biology, National Institute of Biology, Ljubljana, Slovenia (CJFVN); and Department of Ophthalmology, Fondation Asile des Aveugles, Jules-Gonin Eye Hospital, University of Lausanne, Lausanne, Switzerland (ROS)

## Summary

Endothelial cells (ECs) form a precisely regulated polarized monolayer in capillary walls. Vascular endothelial growth factor-A (VEGF-A) induces endothelial hyperpermeability, and VEGF-A applied to the basolateral side, but not the apical side, has been shown to be a strong barrier disruptor in blood–retinal barrier ECs. We show here that VEGF-A presented to the basolateral side of human umbilical vein ECs (HUVECs) induces higher permeability than apical stimulation, which is similar to results obtained with bovine retinal ECs. We investigated with immunocytochemistry and confocal imaging the distribution of VEGF receptor-2 (VEGFR2) and neuropilin-2 (NRP2) in perinuclear apical and basolateral membrane domains. Orthogonal z-sections of cultured HUVECs were obtained, and the fluorescence intensity at the apical and basolateral membrane compartments was measured. We found that VEGFR2 and NRP2 are evenly distributed throughout perinuclear apical and basolateral membrane compartments in unstimulated HUVECs grown on Transwell inserts, whereas basolateral VEGF-A stimulation induces a shift toward basolateral VEGFR2 and NRP2 localization. When HUVECs were grown on coverslips, the distribution of VEGFR2 and NRP2 across the perinuclear apical and basolateral membrane domains was different. Our findings demonstrate that HUVECs dynamically regulate VEGFR2 and NRP2 localization on membrane microdomains, depending on growth conditions and the polarity of VEGF-A stimulation. (J Histochem Cytochem 70: 557–569, 2022)

## Keywords

apicobasal, endothelial barrier, membrane microdomains, receptors, vascular endothelial growth factor receptor, vascular endothelial growth factor A

## Introduction

Endothelial cells (ECs) form an interface between blood and the surrounding tissue. As such, they are exposed to different microenvironments on their luminal/apical and abluminal/basolateral sides. ECs have a highly polarized phenotype, expressing different proteins and lipids at either membrane domains. The two membrane domains are separated on a molecular

level by tight junction proteins that function together as a fence.<sup>1</sup> ECs respond differently to extracellular cues

Received for publication April 8, 2022; accepted June 28, 2022.

### Corresponding Author:

Ingeborg Klaassen, Ocular Angiogenesis Group, Department of Ophthalmology, Amsterdam UMC location University of Amsterdam, Meibergdreef 15, Room L3-117, 1105 AZ Amsterdam, The Netherlands. E-mail: i.klaassen@amsterdamumc.nl

presented to their luminal vs abluminal side. This has been shown for vascular endothelial growth factor-A (VEGF-A), which induces angiogenesis and vascular permeability in ECs.<sup>2-4</sup> VEGF-A is an important player in the pathobiology of diabetic retinopathy.<sup>5-7</sup> Extracellular VEGF-A binds with high affinity to two receptors, VEGF receptors 1 and 2 (VEGFR1 and VEGFR2). Of these receptors, VEGFR2 is the most prominent signaling receptor in ECs, regulating the vascular permeability effects of VEGF-A.<sup>8</sup>

VEGFR1 protein, but not VEGFR2 protein, is constitutively expressed in blood-neural barrier microvessels of humans and monkeys as has been shown in immunohistochemical studies.<sup>9,10</sup> In contrast, VEGFR2 is only expressed in non-vascular cells in control human retina, whereas VEGFR2 expression is induced in microvessels in humans in diabetic retinopathy and in monkeys after repeated intraocular injections with VEGF-A.<sup>9</sup> Similarly, VEGFR1 expression in vascular cells and non-vascular localization of VEGFR2 have also been described in murine retinal wholemounts.<sup>11</sup> However, other authors describe protein expression of VEGFR2 in rodent ECs that form blood-neural barriers.<sup>4</sup> In general, it is accepted that *in vitro* cultured ECs express VEGFR2 protein.<sup>12-15</sup>

Presently, there is still a limited understanding of the polarized localization of VEGFRs in ECs. Hudson et al.<sup>4</sup> described a predominant basolateral localization of VEGFR2 in brain and retinal microvessels of rodents, and VEGF-A presented to the basolateral side of cerebral and retinal ECs induced permeability in both *in vivo* and *in vitro* models. In contrast, VEGFR1 was reported by the same authors to be predominantly localized at the apical side in rodent blood-neural ECs, and VEGF-A presented to the apical side of cerebral and retinal ECs seems to have a cytoprotective role in both *in vivo* and *in vitro* models.<sup>4</sup> This differential distribution of VEGFRs across EC membrane domains was identified in ECs from brain and retina, but not in lung endothelium.<sup>4</sup> Other authors also noted that basolateral VEGF stimulation is more effective in inducing permeability than apical VEGF stimulation in cultured bovine brain ECs.<sup>16</sup>

To date, not much is known of polarized VEGF-A signaling in ECs isolated from other vascular beds than that of the blood-neural barrier type. A commonly used primary EC subtype in *in vitro* studies is the human umbilical vein EC (HUVEC) phenotype. Cultured HUVECs have a highly polarized secretome.<sup>17</sup> Proteins related to the extracellular matrix and cell adhesion are predominantly secreted to the basolateral medium compartment, whereas nucleic acid-binding proteins, which are most likely related to the cargo of extracellular vesicles, are predominantly secreted to the apical medium compartment.<sup>17</sup> HUVECs in culture express a

large portion (approximately 60%) of VEGFR2 at their cell membrane, where it is available for extracellular VEGF to bind.<sup>14,15</sup> VEGF-A stimulation reduces the total cell surface expression of VEGFR2 in HUVECs up to 3 hr after treatment.<sup>18</sup> The remaining portion of VEGFR2 (approximately 40%) is stored within an intracellular endosomal storage pool, from which there is continuous shuttling and recycling to the plasma membrane, also under non-stimulated conditions.<sup>14,15</sup> Endosomal proteins play a key role in maintaining VEGF-A signaling as they stabilize the internalized VEGF-A-VEGFR2 complex, preventing lysosomal degradation and thereby promoting receptor signaling.<sup>12</sup> At the moment, little is known about the delayed effects of VEGF-A on VEGFR2 protein expression in cultured cells (i.e., days after treatment) and how the VEGFR2 membrane pool on the apical and basolateral domain is affected.

The binding of VEGF-A to VEGFR2 is regulated by VEGFR co-receptors such as neuropilin-1 (NRP1) and neuropilin-2 (NRP2).<sup>19</sup> Neuropilins have been shown to play a key role in vascular permeability, via binding to VEGF-A or to members of the semaphorin family.<sup>20-22</sup> Lack of NRP1 expression in mice reduces VEGF-A-induced vascular permeability,<sup>20</sup> whereas lack of NRP2 expression in mice increases inflammation-induced vascular permeability.<sup>22</sup>

In the present study, we investigated how apical and/or basolateral VEGF-A stimulation regulates HUVEC barrier function. In addition, using an immunocytochemistry approach with cells grown on Transwell inserts and coverslips, we quantitatively assessed the relative distribution of VEGFR2 and the VEGF co-receptor NRP2 over the perinuclear apical and basolateral membrane domains in single cells using high-resolution fluorescence confocal microscopy in the orthogonal z-direction. We investigated VEGFR2 as this receptor is essential for VEGF-A-induced permeability, whereas NRP2 was included as this co-receptor has been relatively little studied despite its abundant expression in cultured HUVECs.<sup>13</sup>

## Methods

### Cell Culture

HUVECs were isolated from umbilical cords (obtained from the Department of Gynecology, Amsterdam UMC, location AMC, Amsterdam, The Netherlands) as described previously.<sup>23</sup> HUVECs were cultured in M199 medium (Gibco; Paisley, UK) supplemented with 10% heat-inactivated human serum (obtained from the Department of Oncology, Amsterdam UMC, location AMC, Amsterdam, The Netherlands), 10% fetal bovine serum (FBS) (Gibco), 1% penicillin-streptomycin

(Gibco), and 1% glutamine (Gibco) and grown on 2% gelatin-coated (Merck Millipore; Darmstadt, Germany) plastic tissue culture plates. Subjects gave informed consent for the use of tissues or serum, and samples were stored anonymously. HUVECs were used at passage 4 and cultured at 37°C in 5% CO<sub>2</sub>. Each experiment was repeated in cells from three different donors.

Bovine retinal ECs (BRECs) were isolated from freshly enucleated cow eyes obtained from the slaughterhouse as described previously.<sup>24</sup> BRECs were cultured on collagen type IV-coated (Sigma-Aldrich; St. Louis, MO) and fibronectin-coated (Merck Millipore) plastic plates and grown in DMEM containing 25 mM HEPES and 4.5 g/l glucose (Lonza; Breda, The Netherlands), supplemented with 10% FBS, 1× non-essential amino acids in minimum essential medium (Gibco), fungizone antimycotic (Gibco), 1% penicillin-streptomycin-glutamine (Gibco), 2 mM L-glutamine (Gibco), and 10 µg/ml hydrocortisone (Sigma-Aldrich). BRECs were used at passage 1 and cultured at 37°C in 10% CO<sub>2</sub>. Each experiment was repeated three times.

ECs were either not stimulated or stimulated with recombinant human VEGF-A<sub>165</sub> (ACROBiosystems; Newark, DE).

### Permeability Experiments

ECs were seeded on coated 24-well Transwell inserts (#662640; 0.33 cm<sup>2</sup>, pore size 0.4 µm; Greiner Bio-One, Kremsmünster, Austria) and grown to confluence. Transwell inserts were coated with 2% gelatin (for HUVECs) or with collagen type IV and fibronectin (for BRECs). Cells were basolaterally stimulated with VEGF-A for 24 hr, followed by a second 24 hr VEGF-A incubation period in fresh medium. On the experimental day, fluorescent tracer molecules, 250 µg/ml of FITC-conjugated dextran (#46945, dextran-FITC, 70 kDa; Sigma-Aldrich), and 50 µg/ml of Cy3-tracer (#PA23001, 766 Da; GE Healthcare, Buckinghamshire, UK) were added to the apical side of the Transwell insert, and samples were collected from the basolateral compartment after 4 hr. Fluorescence intensity of samples was measured using a microplate reader (CLARIOstar; BMG LABTECH, Ortenberg, Germany). The intensity of fluorescence of the basolateral compartment samples was considered to be a measure for permeability and is presented relative to that of the unstimulated control.

### Immunofluorescence Staining

HUVECs grown on fibronectin-coated glass coverslips or Transwell inserts were fixed using 4% paraformaldehyde (Electron Microscopy Sciences; Rockford, IL) for 15 min at room temperature, followed by treatment with

0.15% glycine in Hanks' balanced salt solution (HBSS; Gibco) for at least 15 min at room temperature. ECs were washed with HBSS and stored in HBSS at 4°C until further processing. All the incubation steps with the Transwell inserts were performed under gentle agitation. Samples were incubated in 10% normal donkey serum (Jackson ImmunoResearch; Cambridgeshire, UK) and 0.1% Triton-X-100 (Sigma-Aldrich) for 1 hr in normal antibody diluent (#APG500; ScyTek Laboratories, Logan, UT) at room temperature to block nonspecific background staining. Next, samples were incubated with anti-VEGFR2 antibody (#AF357, 1:100; R&D Systems, Minneapolis, MN) or anti-NRP2 antibody (#AF2215, 1:100; R&D Systems) diluted in normal antibody diluent for 2 hr at room temperature. Primary antibodies were omitted for negative controls. After three washes with HBSS, coverslips were incubated with donkey anti-goat Cy3 (#705-165-147, 1:100; Jackson ImmunoResearch, Suffolk, UK) for 1 hr at room temperature. Coverslips were washed again three times with HBSS and mounted in Vectashield mounting medium containing 4',6-diamidino-2-phenylindole (DAPI) (Vector Laboratories; Burlingame, CA).

### Image Acquisition and Quantification

Samples were imaged using a confocal laser scanning microscope (Leica, SP8, 63× objective) at a z-stack interval of 0.3 µm with settings kept constant between conditions. All images of the same experiment were equally adjusted for contrast.

To quantify protein expression on the apical and basolateral membrane domains, images of at least four different orthogonal sections (XZ or YZ projections) were taken per nucleus and analyzed by ImageJ. A similar-sized region of interest (ROI) was acquired at the apical and basolateral membrane, and the mean intensity was quantified. The total mean intensity of ROIs at the apical membrane was expressed relative to the intensity of the ROIs at the basolateral membrane.

To quantify the total protein expression per image, the confocal images in the z-plane were merged to form a two-dimensional projection (XYZ projection) of the image representing the full depth of the cell culture. The images were imported to ImageJ and the integrated density of the fluorescence signal was measured. This value was normalized to the total number of nuclei observed in the frame and expressed relative to the unstimulated control samples.

### Western Blotting

HUVECs were starved for 4 hr in M199 medium supplemented with 2% heat-inactivated human serum

(starvation medium) and stimulated with VEGF-A for 48 hr in complete HUVEC medium. Cells were lysed in radioimmunoprecipitation assay buffer (Thermo Fisher Scientific; Rockford, IL) supplemented with a protease inhibitor cocktail (Roche; Mannheim, Germany). Equal amounts of protein were denatured in SDS-PAGE sample buffer, resolved on 7.5% or 10% SDS-PAGE gels, and blotted onto nitrocellulose membranes (GE Healthcare). Membranes were blocked with 1:1 TBS:Intercept blocking buffer (LI-COR Biosciences; Lincoln, NE). Incubation with primary antibodies was performed overnight at 4°C, followed by incubation with secondary antibodies for 1 hr at room temperature. VEGFR2 was detected with an antibody from Cell Signaling Technology (#2479, 1:1000; Cell Signaling Technology, Leiden, The Netherlands), NRP2 was detected with an antibody from R&D Systems (#AF2215, 1:1000), and  $\beta$ -actin was detected with an antibody from Sigma-Aldrich (#A5441, 1:5000). Proteins were visualized using the Odyssey system (LI-COR Biosciences). Protein bands were analyzed by densitometric analysis using ImageJ.

### Statistics

Data are represented as mean  $\pm$  standard error of the mean (SEM). Data were tested for normality with a Shapiro–Wilk test, and depending on the outcome, a parametric or non-parametric test was performed. Two-group comparisons were analyzed using an unpaired, two-tailed, Student's *t*-test (parametric test), a Mann–Whitney *U*-test (non-parametric), or a Welch's *t*-test when comparisons were made against a normalized control. Differences between multiple groups were analyzed using a one-way analysis of variance (ANOVA; parametric) or a Kruskal–Wallis test (non-parametric), followed by Dunnett's or Dunn's multiple comparisons test to compare with the untreated control condition, respectively. Statistical analyses and graphing were performed using GraphPad Prism 9. *P* values <0.05 were considered to indicate significant differences, with levels of significance as follows: \**p*<0.05; \*\**p*<0.01; \*\*\**p*<0.001.

## Results

### Basolateral VEGF-A, But Not Apical VEGF-A, Induces Endothelial Permeability in BREC and HUVEC Cultures

First, we repeated the experiments of Hudson et al.<sup>4</sup> and Wang et al.<sup>16</sup> in our *in vitro* BREC culture model. We tested the effects of two different concentrations of VEGF-A (25 ng/ml and 100 ng/ml) on the barrier

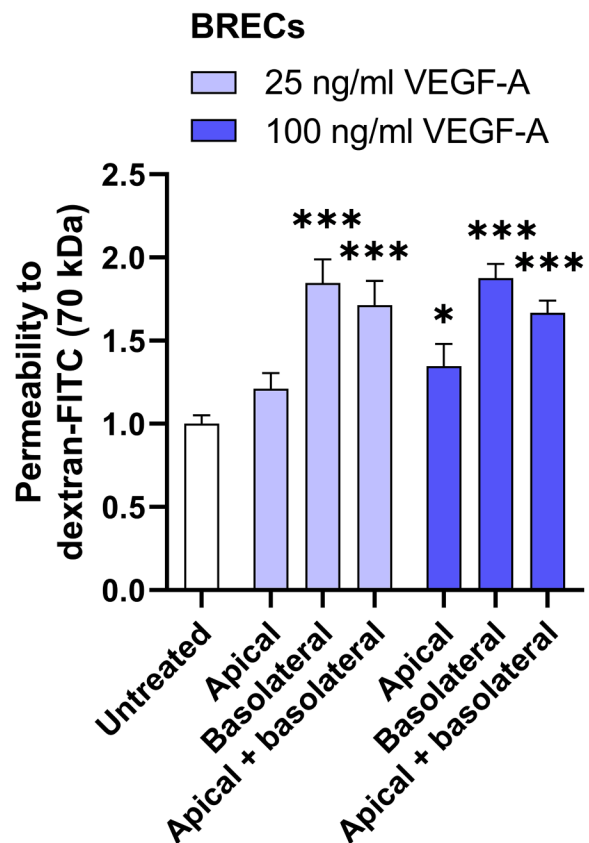


**Figure 1.** Basolateral VEGF-A induces permeability more effectively than apical VEGF-A in BREC cells. Relative permeability to dextran-FITC is shown in BREC cells after apical and/or basolateral stimulation with VEGF-A (25 ng/ml or 100 ng/ml) for 48 hr. Data are normalized to the untreated condition. *n*=8–12 Transwell inserts from three independent experiments. One-way ANOVA followed by Dunnett's multiple comparisons test was used to compare with untreated controls. \**P* < 0.05, \*\*\**P* < 0.001. Abbreviations: VEGF-A, vascular endothelial growth factor-A; BREC, bovine retinal endothelial cells.

functions of BREC cells and measured permeability after VEGF-A treatment for 48 hr. VEGF-A applied to the apical side of the Transwell insert did not alter permeability for 70 kDa dextran when used at 25 ng/ml, but increased permeability for 70 kDa dextran when used at 100 ng/ml by 1.3-fold (Fig. 1). In contrast, basolateral application of VEGF-A increased permeability to 70 kDa dextran by 1.8-fold when used at 25 ng/ml and by 1.9-fold when used at a concentration of 100 ng/ml (Fig. 1). When VEGF-A was presented to the cells on both sides, permeability to 70 kDa dextran was increased by 1.7-fold with both VEGF-A concentrations (Fig. 1). In addition, we also tested permeability to a small 766 Da tracer in BREC cells, but we were unable to draw conclusions because there was large variation across different experiments (data not shown). In summary, the results with 70 kDa dextran confirm previous

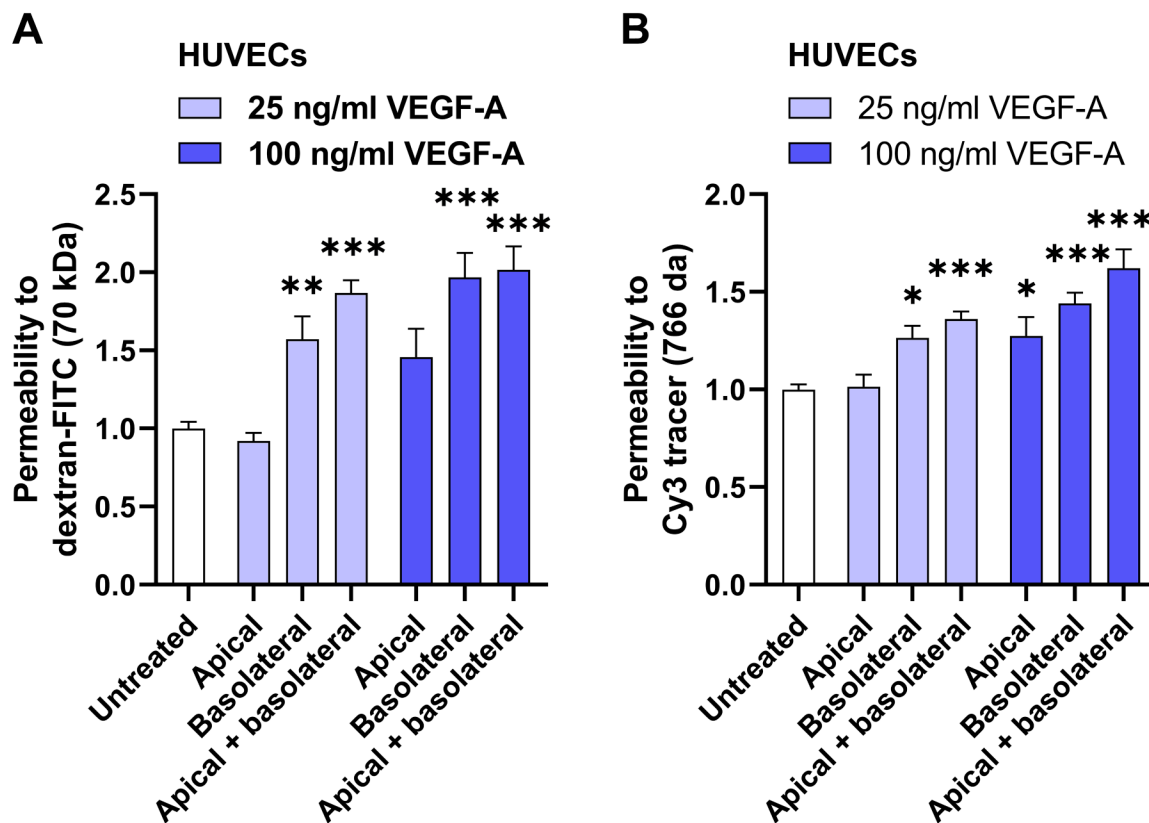


**Figure 2.** Basolateral VEGF-A induces permeability more effectively than apical VEGF-A in HUVECs. Relative permeability to dextran-FITC (A) and 766 Da Cy3 tracer (B) is shown in HUVECs after apical and/or basolateral stimulation with VEGF-A (25 ng/ml or 100 ng/ml) for 48 hr. Data are normalized to the untreated condition.  $n=9-11$  Transwell inserts from three independent experiments. One-way ANOVA followed by Dunnett's multiple comparisons test (A) or Kruskal-Wallis test, followed by Dunn's multiple comparisons test (B) was used to compare with untreated controls. \* $P < 0.05$ , \*\* $P < 0.01$ , \*\*\* $P < 0.001$ . Abbreviations: VEGF-A, vascular endothelial growth factor-A; HUVECs, human umbilical vein endothelial cells.

studies suggesting that basolateral VEGF-A causes more prominent barrier disruption than apical VEGF-A in blood-retina barrier (BRB) ECs.

Next, we tested permeability for 70 kDa dextran in HUVECs challenged with apical and/or basolateral VEGF-A. Apical VEGF-A at a concentration of 25 ng/ml and 100 ng/ml had no effect on the barrier function in HUVECs (Fig. 2A). Basolateral VEGF-A stimulation induced permeability to dextran by 1.6-fold when used at a concentration of 25 ng/ml and by 2-fold when used at a concentration of 100 ng/ml (Fig. 2A). VEGF-A stimulation on both the apical and basolateral side induced permeability to dextran by 1.9-fold and 2.0-fold when used at 25 ng/ml and 100 ng/ml, respectively (Fig. 2A). Similar responses on permeability of apical VEGF-A and basal VEGF-A stimulation were also found with the smaller tracer of 766 Da (Fig. 2B). Taken together, basolateral VEGF-A stimulation is more effective in inducing permeability in HUVECs than apical stimulation.

#### Quantitative Assessment of VEGFR2 and NRP2 Receptor Distribution on Perinuclear Apical and Basolateral Membrane Domains in HUVECs

The polarized response to VEGF-A in HUVECs may be explained by differences in receptor localization as described for BRB ECs.<sup>4</sup> Therefore, we studied the distribution of VEGFR2 and the VEGF co-receptor NRP2 on the different membrane microdomains in HUVECs using confocal imaging. ECs are in general much more flattened compared with other eukaryotic cells. Therefore, only the area around the nucleus was used to determine whether the receptor is localized on the apical or basolateral membrane domain. HUVECs grown on a Transwell insert were stained for VEGFR2 or NRP2, and subsequently large z-stacks were acquired. Representative orthogonal z-sections of the staining in HUVECs are shown in Fig. 3A and C. Immunofluorescence images revealed that there was

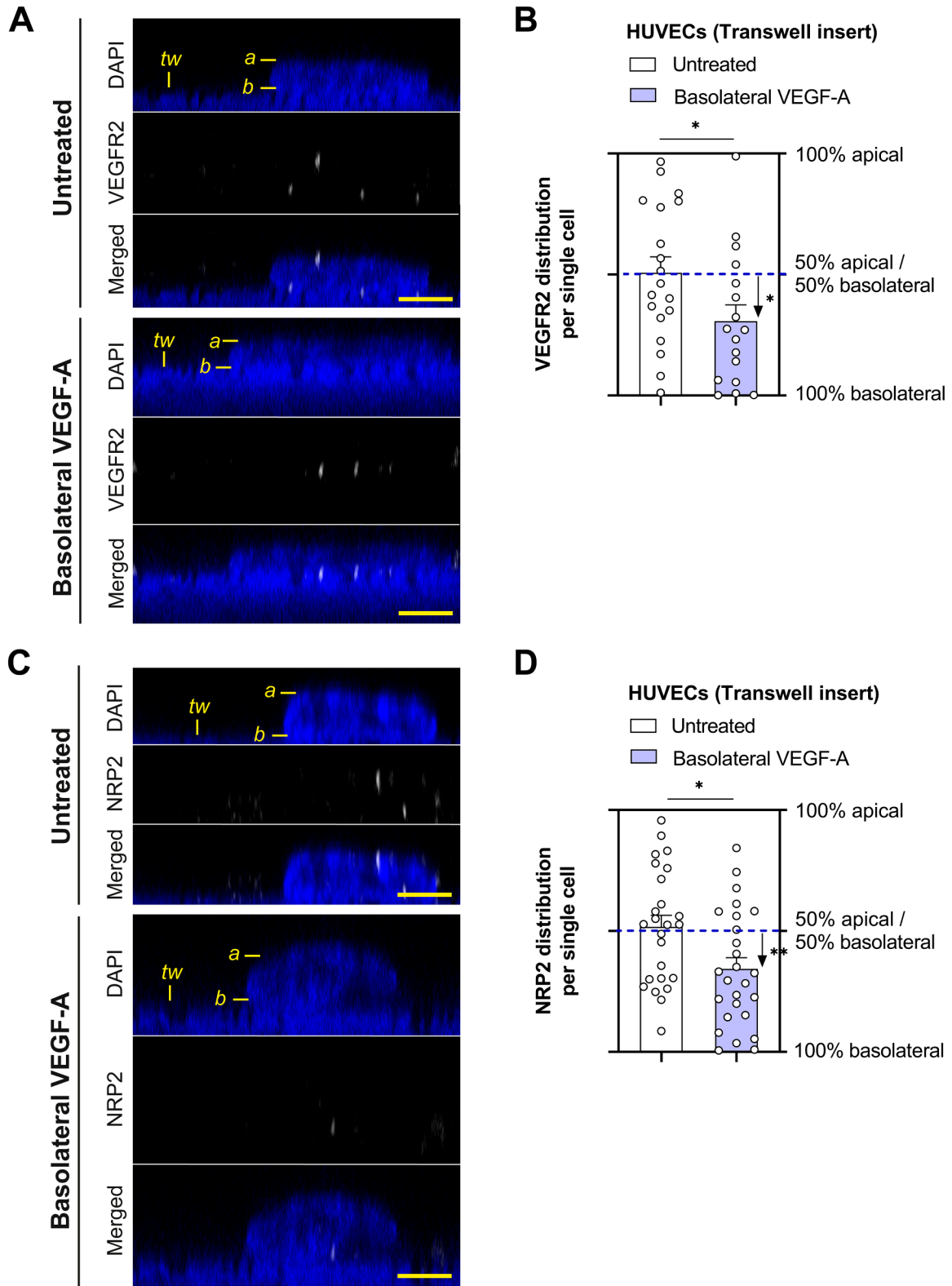


Figure 3. (continued)

**Figure 3.** VEGFR2 and NRP2 distribution in HUVECs cultured on Transwell inserts. Representative orthogonal images of VEGFR2 (A) and NRP2 (C) staining in HUVECs grown on Transwell inserts after stimulation with VEGF-A (25 ng/ml for 48 hr). DAPI staining was used to identify the cell nucleus, but the translucent Transwell inserts showed positivity for DAPI as well. Labeling in the images: *a* marks the apical membrane, *b* marks the basolateral membrane, and *tw* marks the Transwell insert. Quantification of the subcellular signal distribution is shown in (B) and (D).  $n=17-26$  cells from three different donor experiments. Welch's *t*-test was used to test whether there is a preference to apical or basolateral localization within one condition. Student's *t*-test was used to investigate differences between conditions. \* $P < 0.05$ . Scale bars, 5  $\mu$ m. Abbreviations: HUVECs, human umbilical vein endothelial cells; VEGF-A, vascular endothelial growth factor-A.

no preference of VEGFR2 and NRP2 for the perinuclear apical or basolateral membrane domains in untreated HUVECs grown on a Transwell insert (Fig. 3B and D). However, when HUVECs had been basolaterally stimulated with 25 ng/ml VEGF, the majority of VEGFR2 and NRP2 was localized on the basolateral membrane domain (Fig. 3B and D). This suggests that HUVECs dynamically regulate the subcellular localization of VEGFR2 and NRP2, depending on the microenvironment and presence of VEGF-A.

VEGFR2 and NRP2 staining was also performed on cells grown on coverslips. The majority of VEGFR2 was localized around the nucleus at the apical side in untreated HUVECs grown in these conditions, and addition of exogenous VEGF-A to the medium did not alter the distribution (Fig. 4A and B). In contrast, there was no preference of NRP2 to the perinuclear apical or basolateral membrane in untreated HUVECs grown on coverslips, whereas apical VEGF stimulation promoted apical NRP2 localization (Fig. 4C and D).

#### Quantitative Assessment of Total VEGFR2 and NRP2 Protein Expression in HUVECs

In addition to the analysis of protein expression on the different membrane domains, the total expression of VEGFR2 and NRP2 were also analyzed in the same set of images. There was an increase in total VEGFR2 protein expression after basolateral VEGF-A stimulation in HUVECs grown on Transwell inserts, whereas there was no difference in total VEGFR2 protein expression after VEGF-A treatment in HUVECs grown on coverslips (Fig. 5A–D). It should be noted that the responses with HUVECs grown on Transwell inserts were not uniform across all individual donors, and there was no increase in VEGFR2 protein expression after basolateral VEGF-A stimulation in one of the three HUVEC donors (Fig. 5B). The total expression level of VEGFR2 was also quantified in three other HUVEC donors grown on plastic plates. Western blot analysis showed that VEGF-A stimulation does not alter total VEGFR2 protein levels (Fig. 5E and F). Total NRP2 expression was not different between untreated and VEGF-A-stimulated HUVECs grown on Transwell inserts, coverslips, and plastic plates (Fig. 6A–F).

#### Discussion

In the present study, we demonstrate that stimulation of the basolateral compartment with VEGF-A induces higher permeability effects in HUVECs and BRECs than when the apical compartment is stimulated. This suggests that the polarized response to VEGF-A is not specific for BRB ECs, but a more general phenomenon in ECs, at least in *in vitro* models. The polarized response to VEGF-A may also occur in cultured human dermal microvascular ECs, as these cells showed a robust response to basolateral VEGF-A applied at a concentration of 25 ng/ml of VEGF-A (our unpublished observations). Nevertheless, the concentration of VEGF-A generally used in *in vitro* studies is still much higher than VEGF-A levels observed in the *in vivo* situation in patients with VEGF-A-driven disease. For instance, in patients with diabetic macular edema, the VEGF concentration in the vitreous is in the 20–12,600 pg/ml range.<sup>25</sup> In addition, this study underscores that it is possible to perform quantification of proteins across perinuclear apical and basolateral membrane domains of cultured cells using immunocytochemistry and confocal imaging, which has not been performed often.

These findings with respect to polarized permeability responses are not unexpected, as VEGF-A is in general produced in tissues on the basolateral side of the endothelium, whereas levels of VEGF-A in the circulation are extremely low and tightly regulated.<sup>26,27</sup> The polarized response to VEGF-A is in line with what occurs during pathological BRB loss or during angiogenesis. ECs “sense” tissue-resident VEGF produced by hypoxic cells on their basolateral side, and become hyperpermeable or grow toward the signal and form a new blood vessel.

We performed immunocytochemical staining of VEGFR2 and NRP2 in HUVECs grown on Transwell inserts, followed by quantification of apicobasal distribution with ImageJ. We showed that HUVECs on Transwell inserts dynamically regulate the subcellular distribution of VEGFR2 and NRP2, as a shift toward basolateral receptor localization is detected after basolateral VEGF-A stimulation. The detected degree of polarization in receptor localization after VEGF-A stimulation was similar for VEGFR2 and its co-receptor

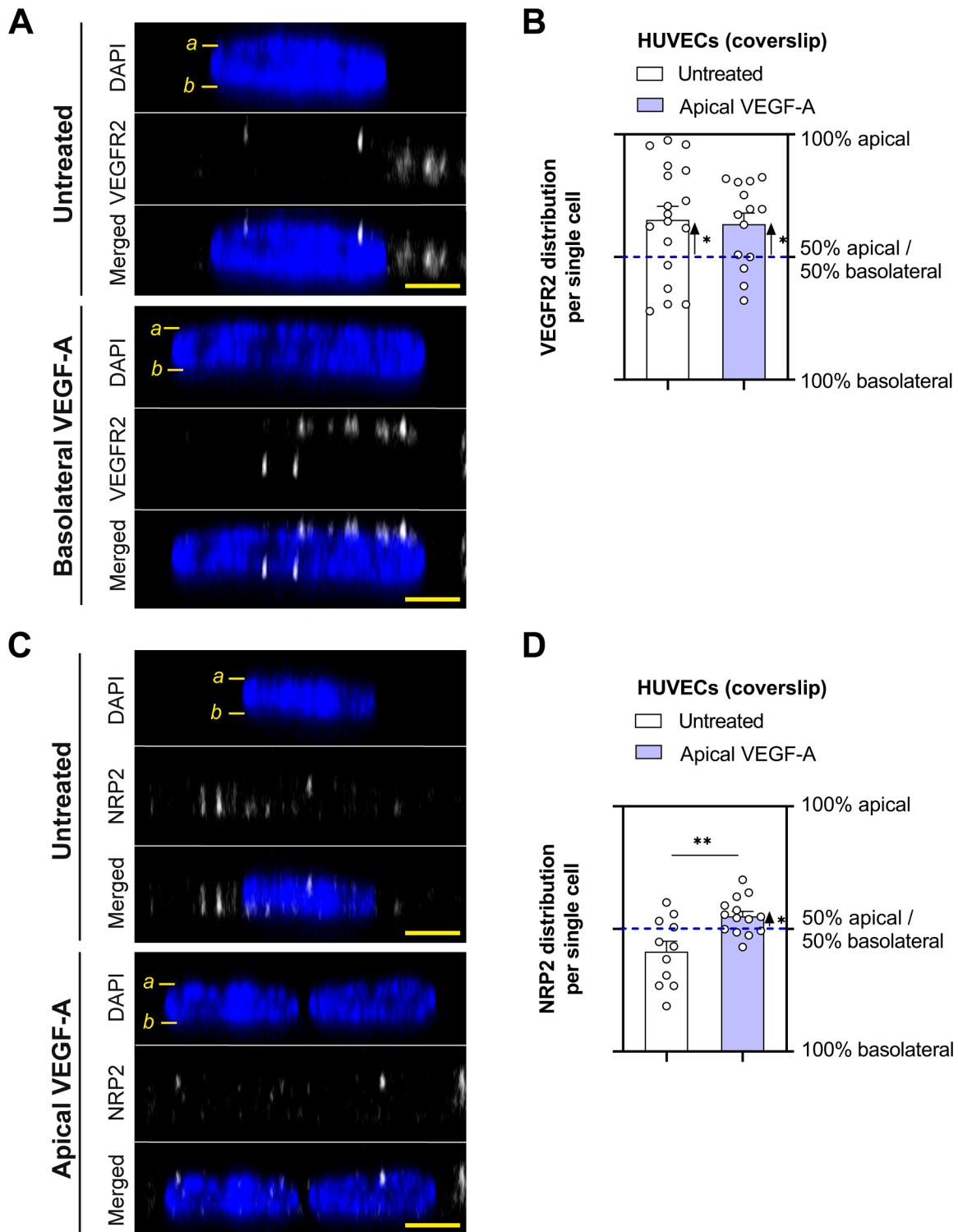


**Figure 4.** VEGFR2 and NRP2 distribution in HUVECs cultured on coverslips. Representative orthogonal images of VEGFR2 (A) and NRP2 (C) staining in HUVECs grown on coverslips after stimulation with VEGF-A (25 ng/ml for 48 hr). DAPI staining was used to identify the cell nucleus. Labeling in the images: *a* marks the apical membrane and *b* marks the basolateral membrane. Quantification of the subcellular signal distribution is shown in (B) and (D).  $n=11-18$  cells from three different donor experiments. Welch's *t*-test was used to test whether there is a preference to apical or basolateral localization within one condition. Student's *t*-test was used to investigate differences between conditions. \* $P < 0.05$ , \*\* $P < 0.01$ . Scale bars, 5  $\mu\text{m}$ . Abbreviations: HUVECs, human umbilical vein endothelial cells; VEGF-A, vascular endothelial growth factor-A.



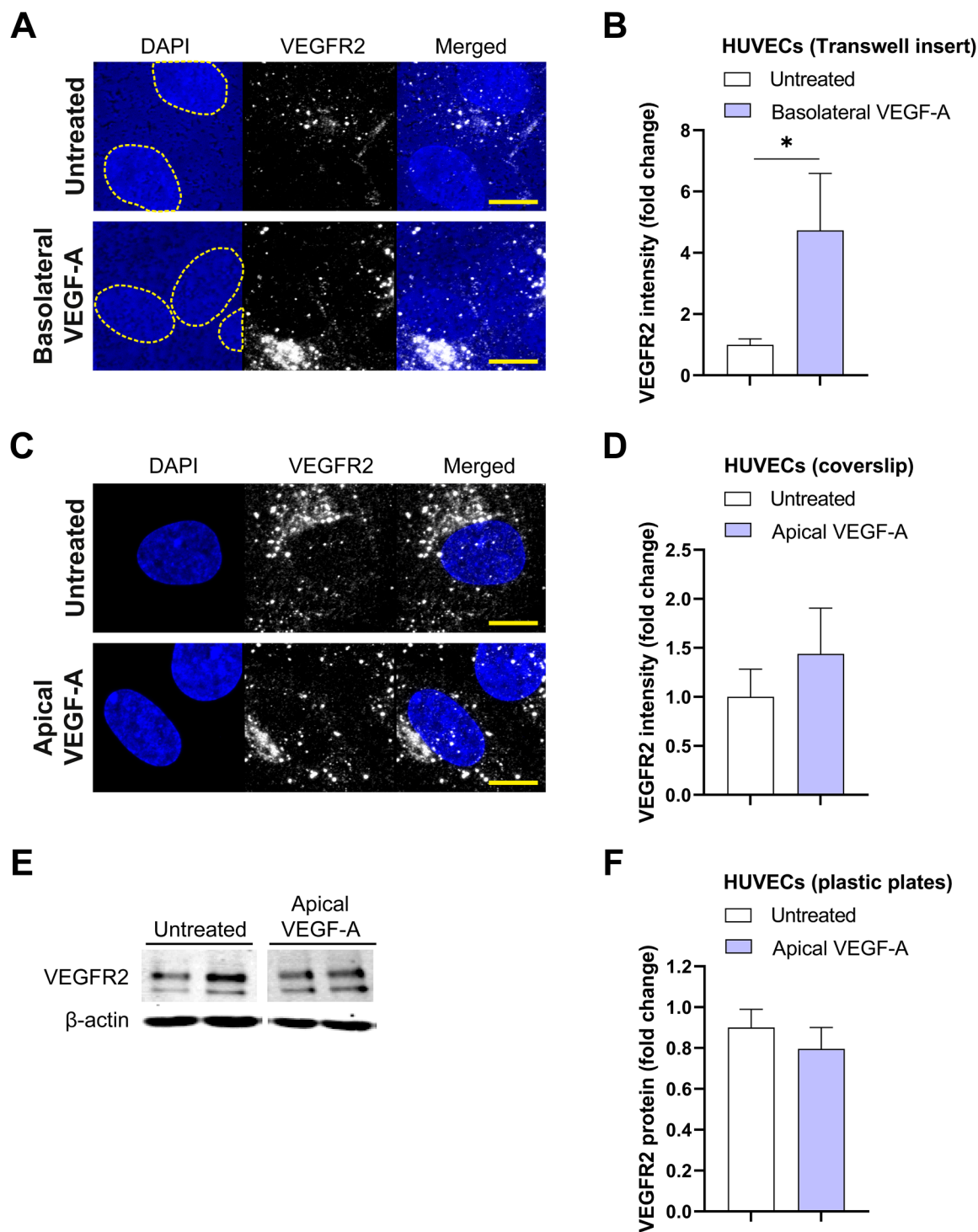


**Figure 5.** Total VEGFR2 protein expression in HUVECs. (A and C) Representative merged projection images of VEGFR2 staining in HUVECs grown on Transwell inserts (A) and coverslips (C) after stimulation with VEGF-A (25 ng/ml for 48 hr). DAPI staining was used to identify the cell nucleus, but the translucent Transwell inserts showed positivity for DAPI as well. A yellow dotted line demonstrates boundaries of cell nuclei in the DAPI channel. Quantification of the fluorescence signal is shown in (B) and (D). Representative Western blots of VEGFR2 and actin (loading control) protein expression after stimulation with VEGF-A (25 ng/ml for 48 hr) are shown in (E). Quantification of Western blot data is shown in (F). (B)  $n=7-10$  images of three different donor experiments. (D)  $n=10-13$  images of three different donors experiments. (F)  $n=6$  wells of three independent donor experiments. (B, D) Mann-Whitney  $U$ -test. (F) Student's  $t$ -test.  $*P < 0.05$ . Scale bars, 10  $\mu$ m. Abbreviations: HUVECs, human umbilical vein endothelial cells; VEGF-A, vascular endothelial growth factor-A.

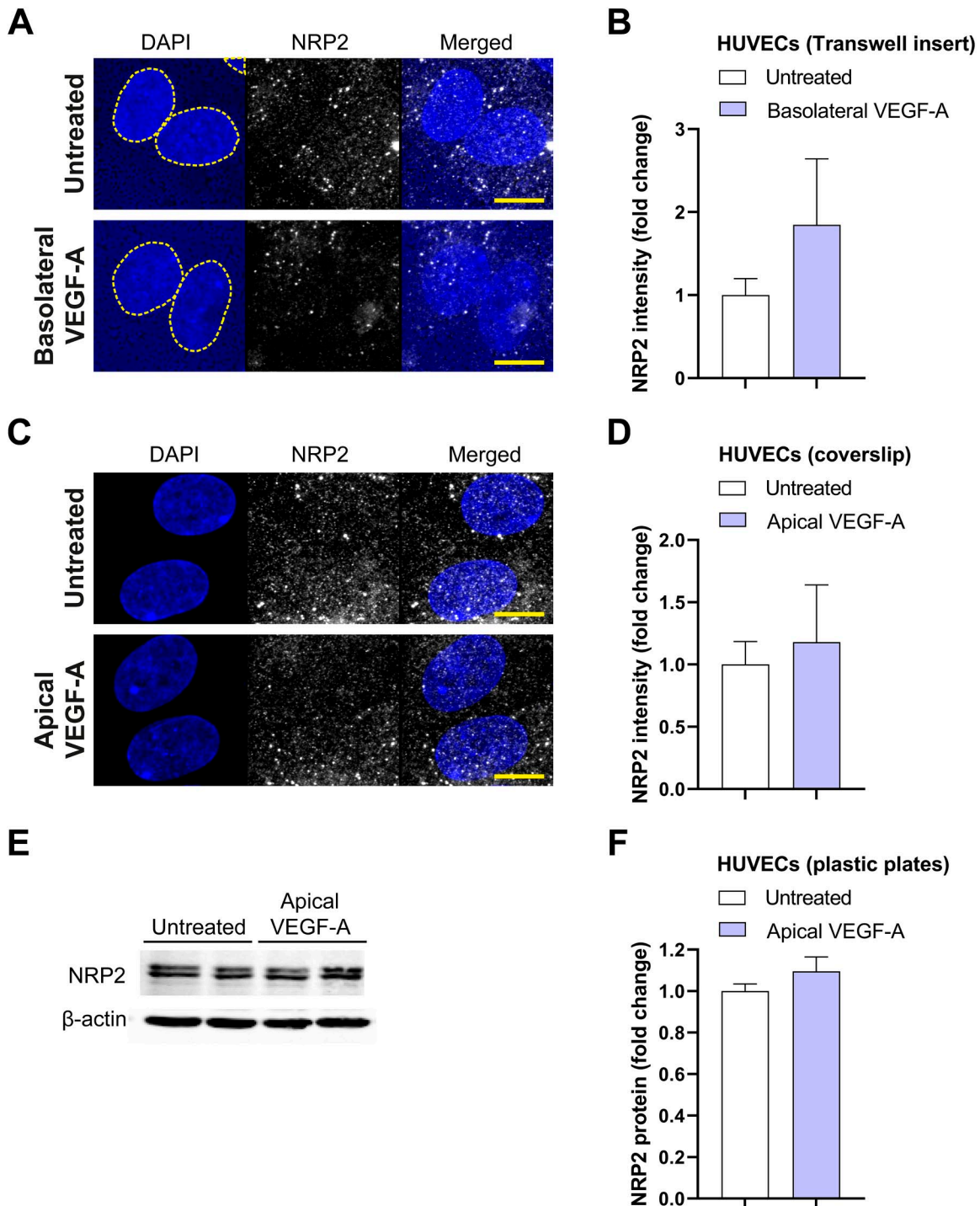


**Figure 6.** Total NRP2 protein expression in HUVECs. (A and C) Representative merged projection images of NRP2 staining in HUVECs grown on Transwell inserts (A) and coverslips (C) after stimulation with VEGF-A (25 ng/ml for 48 hr). DAPI staining was used to identify the cell nucleus, but the translucent Transwell inserts showed positivity for DAPI as well. A yellow dotted line demonstrates boundaries of cell nuclei in the DAPI channel. Quantification of the fluorescence signal is shown in (B) and (D). Representative Western blots of NRP2 and actin (loading control) protein expression after stimulation with VEGF-A (25 ng/ml for 48 hr) are shown (E) and quantified (F). (B)  $n=12$  images of three different donor experiments. (D)  $n=8-9$  images of three different donor experiments. (F)  $n=6$  wells of three different donor experiments. (B, D, F) Mann-Whitney  $U$ -test. Scale bars, 10  $\mu$ m. Abbreviations: HUVECs, human umbilical vein endothelial cells; VEGF-A, vascular endothelial growth factor-A.

NRP2. It remains essential to investigate how HUVECs on Transwell inserts regulate the membrane localization of these proteins after apical VEGF-A stimulation. Moreover, the differences in localization of VEGFR2 and NRP2 in cells grown on Transwell inserts vs coverslips indicates that the microenvironment or accessibility of VEGF-A to the cells is important for membrane localization. It should be noted that the apical membrane compartment is more easily accessible to the antibody solution compared with the basolateral membrane compartment during the staining procedure. Therefore, it is still possible that we are underestimating the basolateral protein expression in our setup.

We also analyzed how VEGF-A treatment affects the total expression levels of VEGFR2 and NRP2 in HUVECs cultured on Transwell inserts, coverslips, and plastic plates at 2 days after stimulation and detected only significant differences in VEGFR2 expression when HUVECs were cultured on Transwell inserts. These differential responses of VEGFR2 expression may be explained by the polarity of stimulation. However, more research is needed to understand how VEGF-A regulates VEGFR2 expression in HUVECs cultured under different conditions. The findings with HUVECs on Transwell inserts are in line with previous *in vivo* studies by our group in monkeys. Repeated VEGF-A injections in the vitreous of monkey eyes, thus to the basolateral side of the endothelium, markedly increased the endothelial expression of VEGFR2 in the BRB and iris.<sup>9,28</sup>

The preliminary results from this study support the hypothesis that there is polarization of VEGFR2 recycling to basolateral membrane domains. This may well explain the strong permeability response to basolateral VEGF-A in activated HUVECs, whereas in resting HUVECs there is no polarized distribution of VEGFR2. A recent study analyzing the polarized secretome of HUVECs described that VEGF, NRP1, and NRP2 are predominantly secreted to the basolateral medium compartment in small interfering RNA (siRNA)-treated control cells.<sup>17</sup> This is comparable to earlier work from our group with epithelial cells that demonstrated polarized basolateral secretion of VEGF in retinal pigment epithelial cells.<sup>29</sup> It is tempting to hypothesize that activated HUVECs predominantly secrete endogenously produced VEGF-A toward the basolateral compartment, and as such promote via an autocrine manner the recycling of internal VEGFR2 to the basolateral membrane, which over time may lead to the hyperresponsive phenotype to exogenous basolateral VEGF-A as shown in this study. Wei et al.<sup>17</sup> also described in their proteomic analysis that VEGFR1, which is probably soluble VEGFR1 (sVEGFR1), is predominantly

secreted to the basolateral medium compartment in untreated HUVECs grown on Transwell inserts. VEGF-A regulates the expression of sVEGFR1 in a VEGFR2-dependent manner, which may function as a negative feedback mechanism to tightly regulate VEGF-A functions.<sup>30</sup> The enrichment of VEGFR1 in the basolateral secretome may be in line with the hypothesis that VEGF-A signaling is more activated at the basolateral side compared with the apical side, and thus requires extra regulators at the basolateral side.

An important open question is how this directional sorting is achieved. It is likely that much can be learned from studying the directional sorting mechanisms that regulate secretion of extracellular matrix proteins or integrins in ECs or from the vast amount of literature on basolateral sorting in epithelial cells.<sup>17,31–33</sup> Our data suggest that the basolateral sorting of VEGFR2 and NRP2 occurs after VEGF stimulation. Therefore, it is interesting to investigate proteins that have been shown to regulate VEGFR2 and NRP2 sorting to the plasma membrane after VEGF stimulation in a polarized experimental setup in future studies.

A limitation of the current study is the small sample size. Nevertheless, our study addresses the apicobasal polarity of VEGFRs in cultured ECs, of which there is currently only a limited understanding. While Hudson et al. studied polarization of VEGFR2 in blood–neural barrier ECs, this is the first study to investigate NRP2 polarity in ECs. To verify our imaging results that estimate protein localization on the different perinuclear membrane domains, quantitative Western blot experiments with cell surface labeling are essential, which take into account larger membrane areas and also include more cells. Further experiments should also investigate the subcellular distribution of other VEGF family members, such as VEGFR1 and NRP1, and investigate phosphorylation of VEGFR2 and other downstream targets to polarized VEGF-A stimulation.

In conclusion, our experiments demonstrate that HUVECs have a polarized (permeability) response to VEGF-A and dynamic regulation of VEGF receptor distribution over the basolateral and apical membranes.

### Competing Interests

The author(s) declared no potential conflicts of interest with respect to the research, authorship, and/or publication of this article.


### Author Contributions

Conceptualization, EKB; methodology, EKB, CJFVN, ROS, IK; formal analysis, EKB; investigation, EKB, SD, JYZ; writing—original draft, EKB; writing—review editing, CJFVN, ROS, IK; visualization, EKB; supervision, IK; funding acquisition, ROS, IK.

## Funding

The author(s) disclosed receipt of the following financial support for the research, authorship, and/or publication of this article: This research was made possible by grants through AMC Foundation (to IK and ROS) and the Slovenian Research Agency (research projects P1-0245 and J3-2526 to CJFVN).

## ORCID iD

Ingeborg Klaassen  <https://orcid.org/0000-0003-1695-9403>

## Literature Cited

- Worzfeld T, Schwaninger M. Apicobasal polarity of brain endothelial cells. *J Cereb Blood Flow Metab.* 2016;36(2):340–62.
- Witmer AN, Vrensen GFJM, van Noorden CJF, Schlingemann RO. Vascular endothelial growth factors and angiogenesis in eye disease. *Prog Retin Eye Res.* 2003;22(1):1–29.
- Dvorak HF, Brown LF, Detmar M, Dvorak AM. Vascular permeability factor/vascular endothelial growth factor, microvascular hyperpermeability, and angiogenesis. *Am J Pathol.* 1995;146(5):1029–39.
- Hudson N, Powner MB, Sarker MH, Burgoyne T, Campbell M, Ockrim ZK, Martinelli R, Futter CE, Grant MB, Fraser PA, Shima DT, Greenwood J, Turowski P. Differential apicobasal VEGF signaling at vascular blood-neural barriers. *Dev Cell.* 2014;30(5):541–52.
- Klaassen I, van Noorden CJF, Schlingemann RO. Molecular basis of the inner blood-retinal barrier and its breakdown in diabetic macular edema and other pathological conditions. *Prog Retin Eye Res.* 2013;34:19–48.
- Bosma EK, van Noorden CJF, Klaassen I, Schlingemann RO. Microvascular complications in the eye: diabetic retinopathy. In: Roelofs JJ, Vogt L editors. *Diabetic nephropathy: pathophysiology and clinical aspects.* Cham: Springer; 2019. p. 305–21.
- Bosma EK, van Noorden CJF, Schlingemann RO, Klaassen I. The role of plasmalemma vesicle-associated protein in pathological breakdown of blood-brain and blood-retinal barriers: potential novel therapeutic target for cerebral edema and diabetic macular edema. *Fluids Barriers CNS.* 2018;15(1):24.
- Simons M, Gordon E, Claesson-Welsh L. Mechanisms and regulation of endothelial VEGF receptor signalling. *Nat Rev Mol Cell Biol.* 2016;17(10):611–25.
- Witmer AN, Blaauwgeers HG, Weich HA, Alitalo K, Vrensen GFJM, Schlingemann RO. Altered expression patterns of VEGF receptors in human diabetic retina and in experimental VEGF-induced retinopathy in monkey. *Invest Ophthalmol Vis Sci.* 2002;43(3):849–57.
- Witmer AN, Dai J, Weich HA, Vrensen GFJM, Schlingemann RO. Expression of vascular endothelial growth factor receptors 1, 2, and 3 in quiescent endothelia. *J Histochem Cytochem.* 2002;50(6):767–77.
- Cao R, Xue Y, Hedlund E, Zhong Z, Tritsarlis K, Tondelli B, Lucchini F, Zhu Z, Dissing S, Cao Y. VEGFR1-mediated pericyte ablation links VEGF and PIGF to cancer-associated retinopathy. *Proc Natl Acad Sci U S A.* 2010;107(2):856–61.
- Kempers I, Wakayama Y, van der Bijl I, Furumaya C, de Cuyper IM, Jongejan A, Kat M, van Stalborch AD, van Boxtel AL, Hubert M, Geerts D, Van Buul JD, de Korte D, Herzog W, Margadant C. The endosomal RIN2/Rab5C machinery prevents VEGFR2 degradation to control gene expression and tip cell identity during angiogenesis. *Angiogenesis.* 2021;24(3):695–714.
- Dallinga MG, Habani YI, Schimmel AWM, Dallinga-Thie GM, van Noorden CJF, Klaassen I, Schlingemann RO. The role of heparan sulfate and neuropilin 2 in VEGFA signaling in human endothelial tip cells and non-tip cells during angiogenesis in vitro. *Cells.* 2021;10(4):926.
- Gampel A, Moss L, Jones MC, Brunton V, Norman JC, Mellor H. VEGF regulates the mobilization of VEGFR2/KDR from an intracellular endothelial storage compartment. *Blood.* 2006;108(8):2624–31.
- Jopling HM, Howell GJ, Gamper N, Ponnambalam S. The VEGFR2 receptor tyrosine kinase undergoes constitutive endosome-to-plasma membrane recycling. *Biochem Biophys Res Commun.* 2011;410(2):170–76.
- Wang W, Merrill MJ, Borchardt RT. Vascular endothelial growth factor affects permeability of brain microvessel endothelial cells in vitro. *Am J Physiol Physiol.* 1996;271(6):C1973–80.
- Wei H, Sundararaman A, Dickson E, Rennie-Campbell L, Cross E, Heesom KJ, Mellor H. Characterization of the polarized endothelial secretome. *FASEB J.* 2019;33(11):12277–87.
- Ewan LC, Jopling HM, Jia H, Mittar S, Bagherzadeh A, Howell GJ, Walker JH, Zachary IC, Ponnambalam S. Intrinsic tyrosine kinase activity is required for vascular endothelial growth factor receptor 2 ubiquitination, sorting and degradation in endothelial cells. *Traffic.* 2016;7(9):1270–82.
- Geretti E, Shimizu A, Klagsbrun M. Neuropilin structure governs VEGF and semaphorin binding and regulates angiogenesis. *Angiogenesis.* 2008;11(3):31–9.
- Fantin A, Lampropoulou A, Senatore V, Brash JT, Prahst C, Lange CA, Liyanage SE, Raimondi C, Bainbridge JW, Augustin HG, Ruhrberg C. VEGF165-induced vascular permeability requires NRP1 for ABL-mediated SRC family kinase activation. *J Exp Med.* 2017;214(4):1049–64.
- Domingues A, Fantin A. Neuropilin 1 regulation of vascular permeability signaling. *Biomolecules.* 2021;11(5):666.
- Mucka P, Levonyak N, Geretti E, Zwaans BMM, Li X, Adini I, Klagsbrun M, Adam RM, Bielenberg DR. Inflammation and lymphedema are exacerbated and prolonged by neuropilin 2 deficiency. *Am J Pathol.* 2016;186(11):2803–12.
- Crampton SP, Davis J, Hughes CCW. Isolation of human umbilical vein endothelial cells (HUVEC). *J Vis Exp.* 2007;3:183.

24. Wisniewska-Kruk J, Hoeben KA, Vogels IMC, Gaillard PJ, van Noorden CJF, Schlingemann RO, Klaassen I. A novel co-culture model of the blood-retinal barrier based on primary retinal endothelial cells, pericytes and astrocytes. *Exp Eye Res.* 2012;96(1):181–90.
25. Shimada H, Akaza E, Yuzawa M, Kawashima M. Concentration gradient of vascular endothelial growth factor in the vitreous of eyes with diabetic macular edema. *Invest Ophthalmol Vis Sci.* 2009;50(6):2953–5.
26. Schlingemann RO, van Noorden CJF, Diekman MJM, Tiller A, Meijers JCM, Koolwijk P, Wiersinga WM. VEGF levels in plasma in relation to platelet activation, glyce-mic control, and microvascular complications in type 1 diabetes. *Diabetes Care.* 2013;36(6):1629–34.
27. Niers TMH, Richel DJ, Meijers JCM, Schlingemann RO. Vascular endothelial growth factor in the circulation in cancer patients may not be a relevant biomarker. *PLoS ONE.* 2011;6(5):e19873.
28. Witmer AN, van Blijswijk BC, van Noorden CJF, Vrensen GFJM, Schlingemann RO. In vivo angiogenic pheno-type of endothelial cells and pericytes induced by vascular endothelial growth factor-A. *J Histochem Cytochem.* 2004;52(1):39–52.
29. Blaauwgeers HG, Holtkamp GM, Rutten H, Witmer AN, Koolwijk P, Partanen TA, Alitalo K, Kroon ME, Kijlstra A, van Hinsbergh VW, Schlingemann RO. Polarized vascular endothelial growth factor secretion by human retinal pigment epithelium and localization of vascular endothelial growth factor receptors on the inner chorio-capillaris. Evidence for a trophic paracrine relation. *Am J Pathol.* 1999;155(2):421–8.
30. Saito T, Takeda N, Amiya E, Nakao T, Abe H, Semba H, Soma K, Koyama K, Hosoya Y, Imai Y, Isagawa T, Watanabe M, Manabe I, Komuro I, Nagai R, Maemura K. VEGF-A induces its negative regulator, soluble form of VEGFR-1, by modulating its alternative splicing. *FEBS Lett.* 2013;587(14):2179–85.
31. Mana G, Clapero F, Panieri E, Panero V, Böttcher RT, Tseng HY, Saltarin F, Astanina E, Wolanska KI, Morgan MR, Humphries MJ, Santoro MM, Serini G, Valdembri D. PPFIA1 drives active  $\alpha 5\beta 1$  integrin recycling and controls fibronectin fibrillogenesis and vascular morpho-genesis. *Nat Commun.* 2016;7:13546.
32. Gonzalez A, Rodriguez-Boulan E. Clathrin and AP1B: key roles in basolateral trafficking through trans-endo-somal routes. *FEBS Lett.* 2009;583(23):3784–95.
33. Thompson A, Nessler R, Wisco D, Anderson E, Winckler B, Sheff D. Recycling endosomes of polarized epithelial cells actively sort apical and basolateral cargos into sep-arate subdomains. *Mol Biol Cell.* 2007;18(7):2687–97.